

Article

Experimental Study of a New Powerful Solar Water Heater

Abderrahmane Diaf^{1*}, Ferhat Kamel Benabdelaziz²

¹ Unité de Développement des Equipements Solaires UDES ; abderrahmane.diaf@yahoo.com

² UDES ; ferhatkamelbenabdelaziz@gmail.com

* abderrahmane.diaf@yahoo.com

Received : 28 June 2022
Accepted : 16 January 2023

Citation : Diaf A. & Benabdelaziz2
F. K. Experimental Study of a New
Powerful Solar Water Heater. *Journal
Algérien des Régions Arides* 2023,
15 (1) : 101–110.

Publisher's Note : ASJP is an
electronic publishing platform for
Algerian scientific journals man-
aged by CERIST, that is not respon-
sible for the quality of content
posted on ASJP.



Copyright: © 2022 by the CRSTRA.
Algerian Journal of Arid Regions is
licensed under a Creative
Commons Attribution
NonCommercial 4.0 (CC BY NC)
license.

Abstract : This study presents a new flat solar heater characterized by a heating power which is considerably higher than that of existing flat systems. The first solar water heater, so-called the “hot box”, was introduced in the late 19th century as a green invention to save on household energy bills. Later on, many other variations of the solar heater entered the market. This work describes the design details and experimental performance data of a new flat solar heater that is simple, cost competitive and capable of delivering a heating power three times higher than that of the currently commercialized conventional systems.

Keywords : Solar heater; water heater; solar collector

1. Introduction

The greenhouse effect was well known and employed for heating by means of collecting and concentrating solar energy way before the advent of the first solar water heater. In fact, in 1869 Mouchot [1] reported on a wide variety of solar thermal applications. Before that, Lonicer in 1551 [2] noted that Arabs Scientists used spherical concave, polished steel mirrors crafted in Damascus and the greenhouse effect to extract essential oils. Then in 1872 the first desalination plant of ocean water using solar distillation by the greenhouse effect was built in Las Salinas, Chile. Technical reports [3, 4] indicate that the plant produced 23 cubic meters of potable water on a site that covered 7900 m². The plant operated continuously for forty years. The “hot box” invention which is considered to be the first solar water heater, was patented in 1891 [5] and entered successfully into commercial production.

Twenty years later, in 1910, the second type of solar water heaters, the Conventional Solar Heater (CSH), a shell and tube heat exchanger type design which was a significant improvement over the “hot box” device, was patented [6] and entered commercial production with great success. Because of its simple design, low cost, ease of installation-operation, no/minimal maintenance and fair performance, it is still in production today in its original shape and form. Although the CSH exhibits many attributes, its shell and tube design makes its heating capability/power inherently limited in applications requiring a robust heating power.

The third innovation in the solar water heater business was the “evacuated solar collector tube”. Numerous patents for example [7-10] among others, were filed/granted for innovations about technical and performance improvements of the vacuum tube solar heater.

The fourth innovation in the flat solar heat collector was “the evacuated flat plate solar collector” which was reported in the literature in 1999 [11]. The authors of the work indicated that the equipment was designed for the production of process steam.

The fifth innovation; which is the topic of this paper, is the tubeless parallel plate solar heater. The idea emerged from development efforts to boost the output of autonomous solar distillation equipments operating with dual heating systems namely; the

greenhouse effect supplemented by flat solar heaters. Since the heating power of the CSH is not high enough, a different type of solar heater, a tubeless design, called the Parallel Plate Collector (PPC) [12], was invented, patented and fabricated for performance evaluation trials. The first key and critical feature of the PPC design is that it has no tubes thus allowing the heating fluid to be in direct contact with the entire surface of the heat absorber exposed to the sun which is significantly higher than that of the CSH. Second, the resistance to flow for the PPC model, which operates on the basis of flow between parallel plates, is lower than that of the tubular flow mode of the CSH. The third major advantage is that the volume of the heating fluid inside the PPC absorber is much larger than that of the CSH. These three key features make the heating power of the PPC considerably higher than that of the CSH.

2. Materials and Methods

2.1. Mechanism of the thermosiphon

Briefly, the thermosiphon phenomenon is a gentle fluid flow process driven by natural free convection. There are no pumps in the system as the whole operation is powered entirely by energy from the sun. In the morning as sunlight impinges on the system, the temperature of the water inside the solar heater starts going up and causing it to rise because of its low density as indicated by arrows 1 and 2 in Figure 1. This natural free convection movement causes cool water from the water tank to be sucked into the solar heater as shown by arrow number 3. As a result, hot water flows naturally into the water tank, arrow number 2 while cooler water flows back into the solar heater, arrow 3, creating a closed loop circulation. In essence this is the process by which heat is transported from the solar heater to the water tank. In the afternoon, the flow stops when the elevation angle of the sun is low enough so as that the incident solar energy is insufficient to keep the water temperature in the solar heater rising.

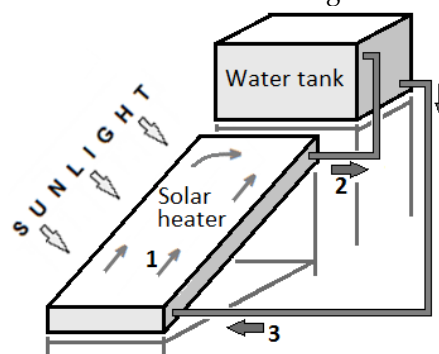


Figure 1. The free convection, natural thermosiphon flow configuration.

2.2. Characteristic features of the CSH

The key component of a solar heater is its heat absorber which in the case of the CSH consists of two elements: The shell with longitudinal grooves shown in Figure 2 (a) and the tube system, Figure 2 (b). The grooved shell is snap-fitted onto the tube system to form the CSH heat absorber, Figure 2 (c). The heat absorber is mounted in a thermally insulated box frame, topped with a transparent cover - glass or plastic. Figure 2 (d) shows the finished product; the commercial CSH used in this study, with its absorber perceptible through the transparent cover.

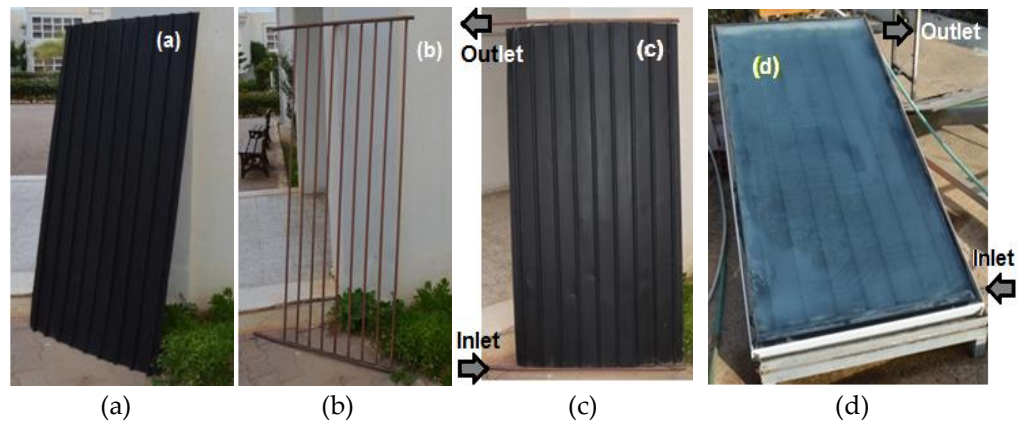


Figure 2. Details of the CSH: Shell (a), tubes (b), absorber (c), commercial CSH (d).

2.3. Design details of the PPC

Similarly, Figure 3 (a) shows a picture of the PPC absorber while Figure 3 (b) shows a picture of the PPC prototype used in the first part of this work.

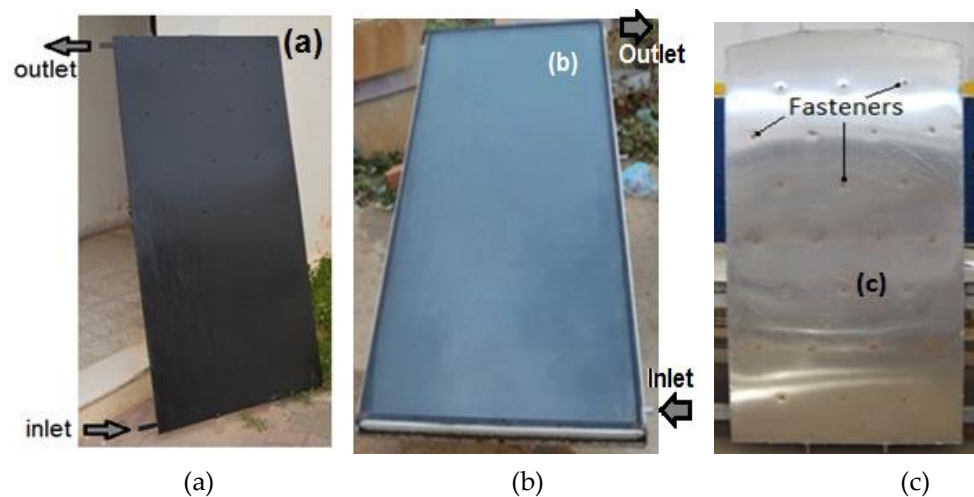


Figure 3. PPC: Heat absorber (a), prototype (b), fasteners (c)

The one-piece, tubeless heat absorber of the PPC consists of two 2 mm thick aluminum sheets, welded together around their perimeters. The gap between the aluminum sheets (for fluid flow) is 4mm which is ensured and fixed by 4 mm thick spacers shown schematically in Figure 4.

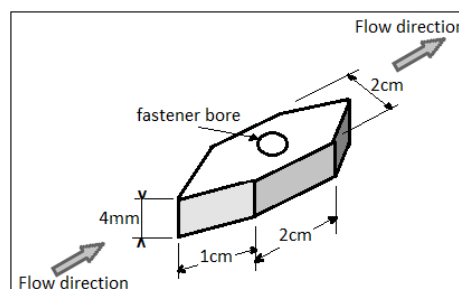


Figure 4. Shape and size of the spacers, their total number is 24

Lower or higher than 4 mm flow clearances may be used depending on design requirements. The absorber sheets are bolted together using 24 screw/nut fasteners with the screws going through the spacers, (fastener bore as shown in Figure 4) to keep a 4mm clearance between the parallel plates for the heating fluid flow. The fasteners are laid out

in a triangular pattern, Figure 3 (c), to prevent bulging of the absorber when filled with water for operation. The side of the solar heat absorber facing the sun is coated with a thin layer of black non-glossy paint as shown in Figure 3 (a).

2.4. Experimental set up

The experimental set up used in this study is shown in Figure 5.

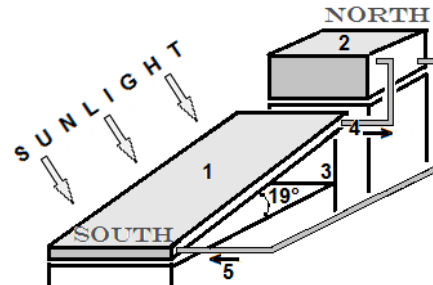


Figure 5. Experimental set up for evaluation of heating power of solar heater.

To ensure similar conditions for performance comparison, the PPC model is a retro-fitted prototype of a commercial flat solar heater whose shell & tube absorber, [shown in Figure 2 (c)], was removed and replaced by the one-piece tubeless PPC heat absorber, [shown in Figure 3 (a)].

2.5. Procedure

For each case study, the solar heater, (1) in Figure 5, is mounted on a metal frame (3) with an inclination angle of 19° with respect to the horizontal plane, at a fixed spot and oriented South using a compass. To carry out experimental evaluations of the heating powers of the CSH and the PPC, the collector is connected to a 110 liter water tank (2), thermally insulated with 5 mm thick of rigid polyurethane foam boards. Three critical temperatures - inside the water tank (2), exit of the solar heat collector (4) and the ambient - are measured at 15 minute intervals with type K thermocouples and recorded via a datalogger. The data acquisition system is set up to cover the whole day; that is 24 hours of continuous operation. All experimental data were collected during the months of July and August. The experimental protocol consisted of setting up the PPC on the support frame (3) then connecting it to the water tank with flexible, garden type hose. The PPC – water tank assembly is filled with tap water introduced from the inlet at the bottom of the PPC (5) to ensure that there is no air trapped inside the PPC. The system is allowed to run for a full day, and then data collection starts immediately thereafter for another day. At the end of the run, the volume of water inside the water tank is measured first, followed by measurement of the volume of water in the PPC.

For performance evaluation of the CSH, the PPC is disconnected and removed from the system. Then the CSH is put in place, on the same supporting frame and the aforementioned procedure is followed to collect the data for the CSH.

3. Results

3.1. The raw data

Three sets of back to back trials were performed with a commercial CSH and the PPC prototype. An example of the temperature versus time raw data as recorded by the datalogger is presented in Table 1.

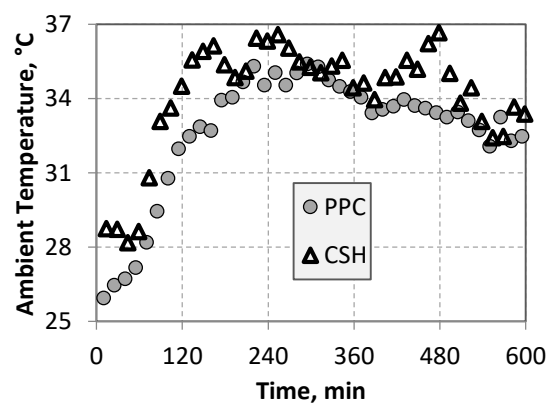
Table 1. Experimental temperature versus time raw data during a PPC trial.

Date	Hour	Time, (min)	Water tank T., (°C)	PPC exit T., (°C)	Ambient T., (°C)
14/07/2020	13:01	594	58,9912	75,7912	35,0438
14/07/2020	13:16	609	60,0417	76,2232	35,4052
14/07/2020	13:31	624	61,0507	77,2035	35,2832
14/07/2020	13:46	639	62,0171	77,1406	34,7567
14/07/2020	14:01	654	63,0671	76,4543	34,4963
14/07/2020	14:16	669	63,6716	76,5633	34,2863
14/07/2020	14:31	684	64,2545	75,9245	34,0546
14/07/2020	14:46	699	64,7206	75,3855	33,4225
14/07/2020	15:01	714	65,0349	74,6168	33,5612
14/07/2020	15:16	729	65,3077	73,8853	33,698
14/07/2020	15:31	744	65,47	72,9647	33,9637
14/07/2020	15:46	759	65,539	71,9704	33,7122
14/07/2020	16:01	774	65,4281	70,2245	33,6194
14/07/2020	16:16	789	65,3981	69,1298	33,428

A common feature of all the performance trials is that the temperature at the exit of the solar heat collector reaches a peak value around 1:30 pm – highlighted in bold numbers in the fourth column of Table 1. Two hours later, the water tank temperature goes through its maximum value, highlighted in bold in column 3.

3.2. Weather conditions

The check for weather is accomplished by visual observation and by recording continuously the ambient temperature. Data recorded on completely clear and calm days are saved and used for the calculation of the heating powers of the CSH and the PPC to ensure similar conditions for comparison. Figure 6 shows the ambient temperature variations that prevailed when testing the CSH on July 8th – data points in bold triangles – and the PPC on July 14th with data points in gray circles. The weather conditions during the comparative trials were fairly similar, although it was rather on the warmer side when the CSH was tested which is acceptable as a worst case scenario.

**Figure 6.** Example of ambient temperature versus time recordings during testing of PPC and CSH

3.3. Comparison of the PPC performance versus the CSH

In order to analyze and highlight the differences in performance between the PPC and the CSH, for convenience, the heating process is divided into three steps: Initiation, operation and termination.

3.3.1. Initiation

The Initiation step begins when the temperature at the exit of the solar collector starts increasing (bold filled circle) as the morning sun shines on the solar heater and ends when the temperature of the water tank starts going up (bold filled square), as illustrated in Figure 7.

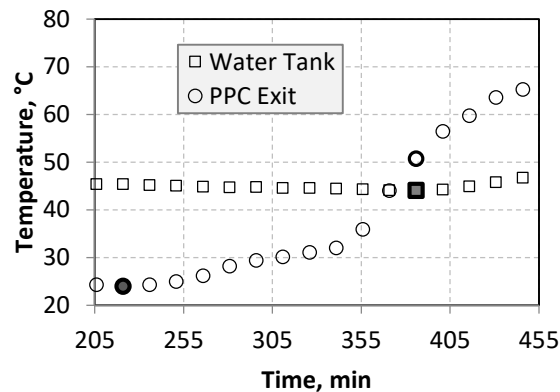


Figure 7. Example of temperature versus time profiles for the PPC at initiation for one trial.

Because of the fact that during initiation there is no/negligible flow in the system, the temperature of the stagnant water inside the solar heater rises fairly quickly. The duration of the initiation step varies depending on the weather conditions, the volume of water inside the solar heater and the efficacy of the solar heater for collecting the incident solar energy. Physically, the end of the initiation step marks the onset of free convection flow in the system that is triggered by a threshold temperature differential ΔT_T between the exit of the solar heater and the water tank as shown in Table 2. As an important note, the reported results in Table 2 represent averages values from six different trials.

Table 2. Average threshold temperature differentials

	ΔT_T , (°C)	Δt , (min)
CSH	8	225
PPC	7	165

The experimental results show that the values of the threshold temperature differential are the same for both the CSH and the PPC. The physical interpretation of this result is that the onset of flow inside the system by natural convection is prescribed by a ΔT of about 7°C between the solar heater and the water reservoir, independently of the nature of the device; PPC or CSH. However, the big difference is the length of time it takes for the system to reach this critical stage. Table 2 reveals that the PPC reaches the threshold ΔT in only 165 minutes while 225 minutes are needed for the CSH. This is due to the fact that the PPC is characterized by a relatively very large solar energy absorbing surface area which is in direct contact with the heating fluid. This is not the case for the CSH. As a result, the PPC “Rate of Solar Energy Absorption”, RSEA as calculated using Equation (1), is 140 Watts compared to only 17 Watts for the CSH as shown in Table 3.

$$RSEA = \frac{m \cdot Cp \cdot \Delta T}{\Delta t} \quad (1)$$

Where: m = Mass of water in the solar collector, grams
 C_p = Specific heat of water, $4.18 \text{ J}\cdot\text{g}^{-1}\cdot(^{\circ}\text{C})^{-1}$
 ΔT = $T_e - T_s$ = Temperature increase of the water inside the collector during the initiation step, $^{\circ}\text{C}$.
 T_e and T_s are the temperatures at the end and the start of the initiation step respectively.
 Δt = $t_e - t_s$ = Time duration of the initiation step, sec.
 t_e and t_s are the times at the end and the start of the initiation step.

Table 3. RSEA values during initiation for the CSH and the PPC

	m , (gram)	T_s , ($^{\circ}\text{C}$)	T_e , ($^{\circ}\text{C}$)	ΔT , ($^{\circ}\text{C}$)	t_s , (sec)	t_e , (sec)	Δt , (sec)	RSEA, (Watts)
CSH	2300	22	46.4	24.4	8100	21600	13500	17
PPC	12400	24	50.7	26.7	13260	23160	9900	140

3.3.2. Operation

Figure 8 shows the evolution of temperature in the water reservoir as a function of time when using the PPC versus the CSH.

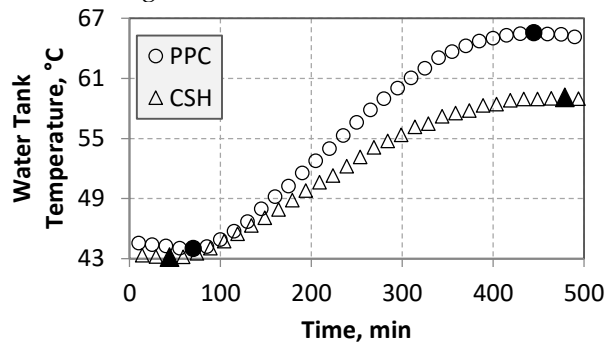


Figure 8. Temperature versus time profiles of the water tank during the Operation step

The operation step is defined as the period that begins when the temperature of the water reservoir starts rising (in the morning as the sun shines on the system) and ends when the temperature reaches a maximum, generally around 2 pm when the sun starts pointing down to dusk. Thus, as illustrated in Figure 8, the operation step covers the time interval between the filled black triangles for the CSH and the filled black circles for the PPC. The duration of the operation step for the CSH is 435 minutes with a temperature rise of 16°C in the water reservoir. As for the PPC, the operation step is 375 minutes with a temperature rise of 22°C , which corresponds to an “Average Heating Power” AHP of 379 Watts for the PPC compared to 192 for the CSH as calculated using equation (2) and reported in Table 4 for the CSH and Table 5 for the PPC.

$$\text{AHP} = \frac{m \cdot C_p \cdot \Delta T}{\Delta t} \tag{2}$$

Where: m = Total mass of water in the system
 C_p = Specific heat of water
 ΔT = Temperature increase from the minimum T_s in the morning, to the maximum T_e in the afternoon
 Δt = Time interval between T_s and T_e

Table 4. Average heating power AHP of the CSH

CSH	m , (kg)	T_s , ($^{\circ}\text{C}$)	T_e , ($^{\circ}\text{C}$)	ΔT , ($^{\circ}\text{C}$)	Absorbed E, tal (kcal)	t_s , (sec)	t_e , (sec)	Δt , (sec)	AHP, (Watts)
Col	2.3	22	64.1	42.1					
Tank	107.5	43.1	59.1	16	1817	8100	47700	39600	192

Table 5. Average heating power AHP of the PPC

PPC	m, (kg)	T _s , (°C)	T _e , (°C)	ΔT, (°C)	Absorbed E, total (kcal)	t _s , (sec)	t _e , (sec)	Δt, (sec)	RSEA, (Watts)
Col	12.4	24	72	48					
Tank	108.9	44	65.5	21.5	2937	13260	45660	32400	379

3.3.2. Termination

Termination is marked by the point at which the temperature of the water tank reaches the maximum value; a point which evidently corresponds also to the end of the operation step. From that point on, the temperature of the whole system gradually decreases as the system cools down due to heat loss to the environment.

3.4. Heating power of a PPC with two inlets and outlets

The objective of this part of the study is to show that the heating power of the solar heater can be improved further by increasing the number of inlets/outlets [13]. Thus, a model with two inlets and outlets (CSP3duo) was fabricated, Figure 9 (a), and tested. The parallel plate construction is conducive to design flexibility to conform specific layout constraints such as shown schematically, for example, in Figure 9 (b) for a Z-type double entry/exit absorber. Systems with 4 inlets/outlets, Figure 9 (c), with a variety of different layouts are also conceivable.

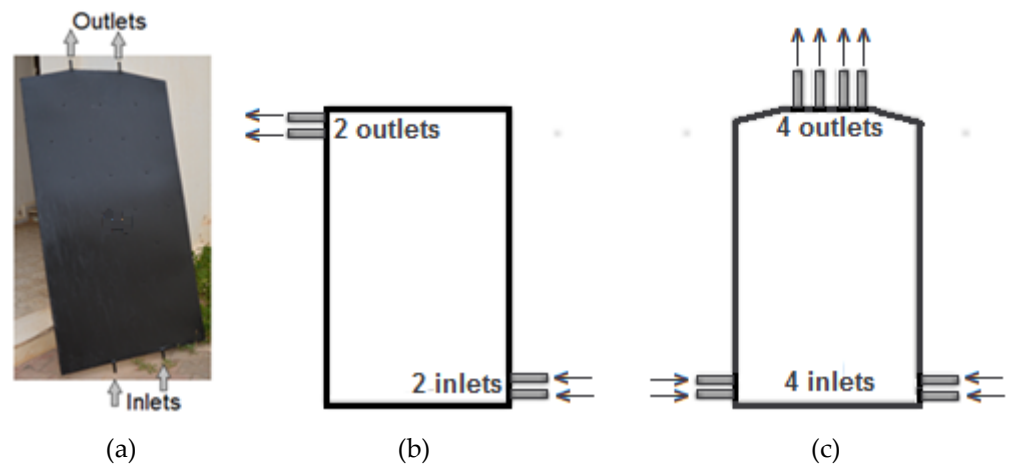


Figure 9. PPC with 2 inlets/outlets (a), Z-shape double inlets/outlets (b), 4 inlets/outlets (c)

Multiple inlets/outlets allow higher flow rates through the absorber, thus increasing heat transport from the solar heater to the water tank. The same aforementioned experimental procedure was followed to evaluate the heating power of the PPCduo. The experimental results of this part of the investigation are summarized in Tables 5, 6 and 7. Table 5 indicates that the amount of Solar Energy Absorbed (SEA) during the “Initiation” phase is the same for the two versions of the PPC which is intuitively correct because of the fact that the two solar heaters are similar in design, shape and size. Therefore, they absorb similar amounts of energy during “Initiation”. The situation changes dramatically during the “Operation” step because of the thermosiphon flow by which heat is transported from the solar heater to the water tank. Table 7 shows the amount of Energy Supplied (ES) by the solar heater to the water tank. Table 8 shows that the Heating Power (HP) of the PPCduo (with 2 inlets and 2 outlets) is 1.5 times higher than that of the regular PPC (with 1 inlet and 1 outlet) when corrected for surface area to take into account the size of the collector.

Table 6. Solar energy absorbed by collector of PPC compared to PPCduo during Initiation

	m, (grams)	To, Col ¹ (°C)	Te Col ¹ (°C)	ΔT, (°C)	SEA, (kcal)
PPC	12400	12.4	51	38.6	478.64
PPCduo	12800	20.2	58.1	37.9	485.12

¹ Col stands for Collector.**Table 7.** Energy supplied to water tank by PPC compared to PPCduo during Operation

	m, (grams)	To, WT ¹ (°C)	Te WT ¹ (°C)	ΔT, (°C)	ES, (kcal)
PPC	114600	28.1	43.8	15.7	1799.22
PPCduo	104200	20.7	52.2	31.5	3282.3

¹ WT stands for Water Tank.**Table 8.** Heating power of the PPC compared to that of the PPCduo

	Total EA ¹ (kcal)	ts, (sec)	tf, (sec)	Δt, (sec)	HP (Watts)	Area (m ²)	HP/m ²
PPC	2277.86	0	29100	29100	327	1.79	182
PPCduo	3767.42	1380	30180	28800	547	2.02	271
Ratio	1.65				1.67		1.48

¹ EA stands for Energy Absorbed by the whole system.

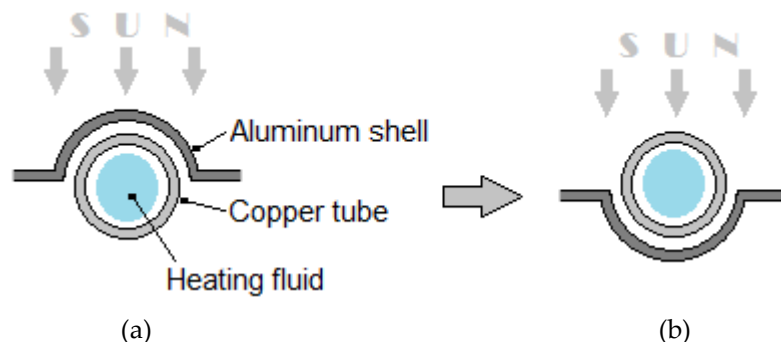
4. Discussion

4.1. On the protection of the environment

Flat solar heaters offer an environmentally clean, simple and inexpensive choice with regards to heating water or other fluids for a very broad diversity of household/commercial/industrial applications. The use of a combination of recyclable, biodegradable and low carbon print materials for the construction of the solar heater, a focus of this work, is evidently a significant plus. As a result, materials such as glass and copper are deliberately avoided. For non-flat solar heaters such as the vacuum tube collector, these devices are more complex and more expensive. Furthermore, the evacuated glass tubes are not recommendable for regions where large hail storms may develop for that would damage completely the device.

4.2. Design-Performance relationships

There are a number of design features of the CSH that need attention but for the sake of conciseness, only a couple will be addressed in this discussion. First of all, the currently available commercial CSH is constructed as represented in Figure 10 (a).

**Figure 9.** Cross section view of CSH: Common configuration (a), more effective (b)

Evidently, the heat transfer mechanism for that configuration is inefficient in that the heat from the sun needs to be conducted through the aluminum shell. In the practical world, the contact between the aluminum shell and the copper tube is not perfect, thus there is a hindrance to a smooth transfer of heat from the shell to the surface of the copper tube. Then, that heat is conducted through the thickness of the copper tube to the heating fluid. The second point is that the heat transfer process to the heating fluid could be enhanced by inverting the absorber as shown in Figure 10 (b). That is actually the configuration that was used to this study to ensure a best case scenario for performance evaluation of the CSH.

The situation with the Parallel Plate Collector design is completely different and better compared to the CSH. As shown in Figure 11, heat from the aluminum sheet is transferred directly to the heating fluid which is in direct contact with the hot aluminum sheet. Furthermore, the surface area exposed directly to the sun and in direct contact with the heating fluid is far greater compared to the CSH. Consequently, there is a huge difference in the heating power of the PPC design compared to the CSH.

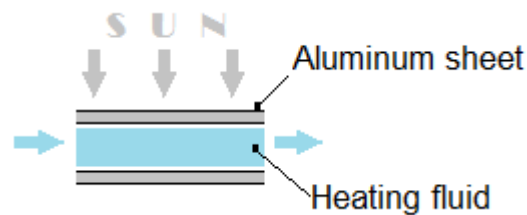


Figure 9. Cross section view of the PPC design

4.3. Cost

Obviously, without going into the details, the PPC design offers a remarkable cost advantage over the CSH and other solar devices used for heating water or other fluids.

5. Conclusions

The Conventional solar heater (CSH) is a practical system for heating water or other fluids using solar energy. The CSH heating power is low which makes its applications limited to low temperature processes. On the other hand, the Parallel Plate Collector (PPC) is a simple, highly cost competitive device characterized by a significantly higher heating power: The experimental results of this study showed that the heating power of the PPC with a single inlet and single outlet is double that of the CSH. The heating power of the PPC can be improved further by providing multiple inlets and outlets to the PPC. Study of a PPC prototype with two inlets and two outlets (PPCduo) showed that its heating power is 1.5 times higher than that of the PPC with one inlet and one outlet.

References

1. Mouchot, A. La chaleur solaire et ses applications industrielles, Gauthier-Villars, 1869
2. Lonicer, A. Naturalis historiae opus novum, apud Chr. Egenolphum (Francfort) 1551
3. Delyannis, E. Historic background of desalination and renewable energies, *solar energy* 2003, 75 (5)
4. Diaz S.G; Haas M.J; Roman L.R. The integration between solar energy and mining in Chile, *Conference proceedings of the Solar World Congress*, 2015
5. Kemp, C. Apparatus for utilizing the sun's rays for heating water, *US Patent US451384*, 1891
6. Bailey, W.J. Solar Heater *US Patent 966,070A*, 1910
7. Novinger, H.E. Evacuated-tube solar collector, *US Patent US4177794A*, 1979
8. McConnell, R.D.; Vansant, J.H. Glass heat pipe evacuated tube solar collector, *US Patent US4,474,170*, 1984
9. Crawmer, D.L. Evacuated tubes for solar thermal energy collection, *US patent US20120204860A1*, 2015
10. Watkins, A.W.; Watkins, I.W. Evacuated Solar Collector Tube, *US Patent US4987883A*, 1988
11. Benz, N.; Beikircher, T. High Efficiency Evacuated Flat Plate Solar Collector for Process Steam Production, *Solar Energy*, 1999, 65, N°2, 111-117
12. Diaf, A.; Sendjakeddine, M. Chauffe-eau Solaire à Plateaux Parallèles, *INAPI patent N°10154*, 2020

13. Diaf, A.; Djebli, A.; Haddad, B. Capteur solaire plan à plateau parallèles à entrées et sorties multiples, *INAPI patent filed N°210730*, 2021